## References

[1] J. J. Gustincic, "A quasi-optical radiometer," in *Dig. Second Int. Conf. Submillimeter Waves and Their Applications*, (San Juan, Puerto Rico), Dec. 1976, pp. 106–107.

[2] J. J. Gustincic, "A quasi-optical receiver design," in *IEEE MTT-S Int. Microwave Symp. Dig.*, 1977, pp. 99–101.

[3] See, for example, M. Born and E. Wolf, *Principles of Optics*. New York: Pergamon, 1965.

[4] N. R. Erickson, "A directional filter diplexer using optical techniques for millimeter to submillimeter wavelength," *IEEE Trans. Microwave Theory Tech.*, vol. MTT-25, pp. 865–866, Oct. 1977.

[5] J. A. Arnaud, A. A. M. Saleh, and J. T. Ruscio, "Walk-off effects in Fabry–Perot diplexers," *IEEE Trans. Microwave Theory Tech.*, vol. MTT-22, pp. 486–493, May 1974.

[6] P. F. Goldsmith, "Diffraction loss in dielectric-filled Fabry–Perot interferometers," *IEEE Trans. Microwave Theory Tech.*, vol. MTT-30, pp. 820–823, May 1982.

[7] N. Nakajima and R. Watanabe, "A quasioptical circuit technology for short-millimeter wavelength multiplexers," *IEEE Trans. Microwave Theory Tech.*, vol. MTT-29, pp. 897–905, Sept. 1981.

[8] A. E. Chiou and H. M. Pickett, "Quasi-optical ring resonator diplexer: Theory and experiment," in *Dig. Sixth Int. Conf. Infrared and Millimeter Waves*, Dec. 1981.

[9] S. R. Barone, "Resonances of the Fabry–Perot laser," *J. Appl. Phys.*, vol. 34, pp. 831–843, Apr. 1963.

[10] G. D. Boyd and J. P. Gordon, "Confocal multimode resonator for millimeter through optical wavelength masers," *Bell. Syst. Tech. J.*, vol. 40, pp. 489–508, Mar. 1961.

[11] M. S. Durschlag and T. A. DeTemple, "Far-IR optical properties of freestanding and dielectrically backed metal meshes," *Appl. Opt.*, vol. 20, no. 7, pp. 1245–1251, Apr. 1981.

[12] C. C. Chen, "Transmission through a conducting screen perforated periodically with apertures," *IEEE Trans. Microwave Theory Tech.*, vol. MTT-18, pp. 627–632, Sept. 1970.


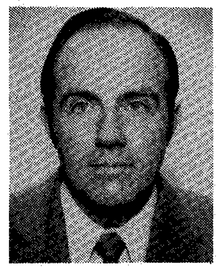

**Herbert M. Pickett** was born in Baltimore, MD, on April 2, 1943. He received the A.B. degree from Williams College in 1965 and the Ph.D. degree in physical chemistry from the University of California, Berkeley, in 1970. From 1970 to 1973 he was a postdoctoral fellow at Harvard with E. Bright Wilson, Jr. In 1973 he was a Miller Fellow at the University of California.

From 1973 to 1978 he was an Assistant Professor at the University of Texas at Austin. Currently, he is a Research Scientist and Supervisor of Submillimeter Development at the Jet Propulsion Laboratory, California Institute of Technology, Pasadena, CA.

**Arthur E. T. Chiou** was born in Bassein, Burma, on January 16, 1947. He received the B.Sc. degree in physics from Rangoon Arts and Science University, Rangoon, Burma in 1968, and the M.S. degree in physics from National Taiwan University, Taipei, Taiwan, Republic of China in 1972. He is expected to receive his Ph.D. degree in applied physics from the California Institute of Technology, Pasadena, CA, in June 1983.

He is currently employed at IBM San Jose Research Laboratory.

# Numerical Analysis of Open-Ended Coaxial Lines

GREGORY B. GAJDA AND STANISLAW S. STUCHLY, SENIOR MEMBER, IEEE

***Abstract*—Numerical methods are applied in the analysis of coaxial structures used as sensors for *in vivo* permittivity studies of biological substances. The methods used for the solution of the resulting static conductor–dielectric problems are the Finite Element Method (FEM) and the Method of Moments (MOM) applied to a pair of coupled integral equations. A linear model which relates the sample permittivity to the fringing field capacitance of the sensor is discussed and values of the model parameters are calculated for different types of sensors.**

Manuscript received June 25, 1982; revised December 29, 1982. This work was supported by grants from the National Sciences and Engineering Research Council of Canada and Health and Welfare Canada.

The authors are with the Department of Electrical Engineering, University of Ottawa, Ottawa, Ontario, Canada, K1N 6N5.

## I. Introduction

OPEN-ENDED coaxial lines have been used extensively as sensors for permittivity measurements of biological substances in recent years [1]. Their simple geometry and small size (potentially as small as 0.5-mm diameter) makes them suitable for *in vivo* measurements as

0018-9480/83/0500-0380$01.00 

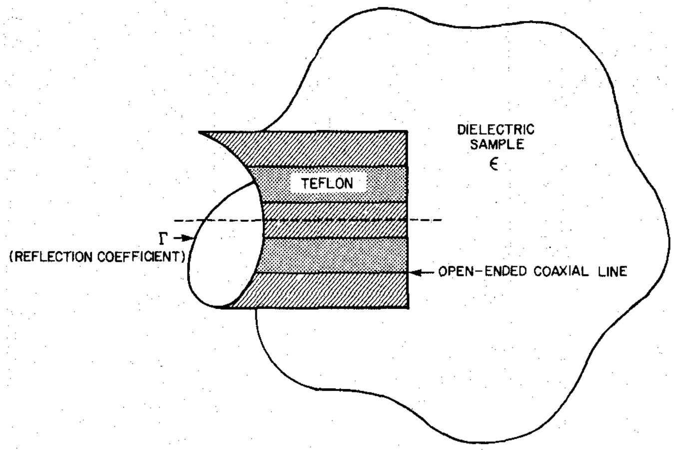


Fig. 1. Open-ended coaxial sensor for dielectric measurement.

well as measurement of the spatial distribution of permittivity. Other advantages of the open-ended coaxial line over other sensor configurations are: a broad frequency range; compatibility with time-domain, applicability to frequency-domain, and resonant measurement techniques; and ease of fabrication.

When used as a sensor for dielectric measurement, the open end of the line is inserted into the sample (as in Fig. 1), and the input reflection coefficient (or input admittance) is measured at a specific frequency and temperature. Various methods have been used to relate the reflection coefficient data to the dielectric properties of the sample. These range from analytical/graphical methods [2], to equivalent circuit approaches and interpolation methods [3].

A solution of the scattering from the open end of a coaxial line in contact with a lossy dielectric was presented by Mosig *et al.* [2]. Nomograms of reflection coefficient versus relative permittivity of the half-space medium were constructed, from which $\epsilon'$ and $\epsilon''$ could be calculated for a given reflection coefficient. A major limitation of this approach is that extensive nomograms are required at each measurement frequency. Also, the numerical computations required to generate the nomograms become increasingly time consuming for high permittivities such as those encountered in biological substances at low frequencies [2].

Several authors have made use of a lumped equivalent circuit, relating the admittance of the sensor to the permittivity. This approach has the advantage that closed-form expressions for $\epsilon'$ and $\epsilon''$ as a function of the reflection coefficient can be derived and used in automatic network analyzer routines. Burdette *et al.* [3] used an equivalent circuit consisting of a single lumped-shunt-capacitance whose effective value was equal to the fringing capacitance of the open-ended line in air multiplied by the sample permittivity. An additional shunt capacitance whose value is independent of the sample permittivity was added in [4] to account for fringing inside the coaxial line. Also, the effect of radiation from the open end on the equivalent circuit was treated by Stuchly *et al.* [5] and used in measurements by Brady *et al.* [6]. In all of the references pertaining to the lumped circuit approach, the equivalent circuit parameters of the sensors were either measured directly or inferred from measurements on known dielectrics. Also, the assumption was made that the fringing capacitances are linearly proportional to the permittivity and independent of frequency.

The purpose of this work is to use numerical methods to investigate the behavior of the fringing capacitance of coaxial sensors, shown in Fig. 1, as a function of the sample permittivity. In particular, the two-capacitance or linear model, relating the net fringing capacitance to the permittivity, is examined.

Since it is known [7]–[9] that the fringing capacitance for the homogeneous case is constant from dc to microwave frequencies (for all practical sizes of line), only the static fringing capacitances are calculated in the present work. The two numerical methods selected to solve the resulting static conductor–dielectric problems are the Finite Element Method (FEM) and the Method of Moments (MOM) applied to a pair of coupled integral equations. Since all solutions are for the static case, only lossless dielectric are modelled.

## II. Theory

### A. Capacitance Model

For the purposes of presentation of the numerical results, a linear model relating the net fringing capacitance to the permittivity $\epsilon$ is assumed. The fringing capacitance may be written as

$$C(\epsilon) = C_f + \epsilon C_0 \tag{1}$$

where $\epsilon$ is the relative permittivity of the sample occupying the space outside the line (Fig. 1).

This is the form of $C(\epsilon)$ used by a large number of investigators [1]. The constant term $C_f$ may be considered to represent storage of energy in the fringing fields inside the line while the linear term $\epsilon C_0$ represents energy storage in the dielectric.

For the case where the sample dielectric is air ($\epsilon = 1$), the net fringing capacitance is equal to the algebraic sum of $C_f$ and $C_0$

$$C(1) = C_f + C_0 = C_T \tag{2}$$

where the value of $C(1)$ is designated the total capacitance $C_T$. This quantity is readily measured, or, for the homogeneous case (i.e., for an air line), it may be calculated from a formula given in [8].

Numerical methods are used to calculate values of the net fringing capacitance $C(\epsilon)$ for each assumed value of $\epsilon$. From this data, values of $C_f$ and $C_0$ can be calculated for each $\epsilon$ by solving the simultaneous linear equations (1) and (2). In general, both $C_f$ and $C_0$ will be functions of $\epsilon$ if $C(\epsilon)$ varies nonlinearly with $\epsilon$; however, if a range of $\epsilon$ exists where $C_f$ and $C_0$, calculated in the above manner, are constant, the linear model will be approximately valid over this range.

### B. Numerical Methods

*1) Finite Element Method:* The two-dimensional FEM was used to solve Laplace's equation indirectly in the rotationally symmetric region of Fig. 2, representing the open end of a coaxial line. The region which is partially bounded by Dirichlet and homogeneous Neumann boundaries was divided into triangular elements. In each element, the permittivity $\epsilon_t$ is known and the unknown potential $\phi$ is approximated by a polynomial trial function with constant coefficients. The trial functions were substituted into the variational expression

$$F=\int_R \epsilon(\nabla\phi)^2\,dR \tag{3}$$

$$=\sum_{t}^{\text{No. T.}} \epsilon_t \int_{R_t} (\nabla\phi)_t^2\,dR \tag{4}$$

which is proportional to the stored energy in the system, and (4) was minimized with respect to the unknown constant coefficients. This procedure produced a system of algebraic equations for the unknown coefficients which can be solved by standard methods.

It can be shown that the continuity of the normal flux between adjacent dielectric regions (interface conditions) are satisfied as a result of minimizing the variational expression [4], [10].

Since the problem is unbounded in the positive $z$-direction, an approximate Neumann boundary representing fringing electric field line is used to close the region of solution. The position of the approximate boundary is first assumed and later, as solutions are run, it is further refined. The criterion used for determining a sufficient size for the half-space region in Fig. 2 was the convergence of the total stored energy.

*2) Method of Moments:* The MOM was used to solve for the unknown charge distribution on the conductor and dielectric interface surfaces shown in Fig. 2. The coupled integral equations which relate the free and bound surface charge densities $\sigma(s)$ residing on conductors and dielectric interfaces, respectively, to the potential distribution $\phi(s)$ are given by [11]

$$\int_{S_c+S_I} \sigma(s')G(s|s')\,ds'=\phi(s), \qquad s \text{ on } S_c \tag{5}$$

$$\frac{\epsilon_1+\epsilon_2}{2}\sigma(s)+(\epsilon_1-\epsilon_2)\int_{S_c}\sigma(s')\frac{\partial G}{\partial n}(s|s')\,ds'=0, \qquad s \text{ on } S_I \tag{6}$$

where $G(s|s')$ is the free-space potential Green's function and $S_c$ and $S_I$ denote conductor and interface surfaces, respectively.

The two permittivities $\epsilon_1$ and $\epsilon_2$ correspond to the two dielectric regions and the normal $n$ is directed from region 1 to region 2 as in Fig. 3.

In rotationally symmetric systems, the free-space Green's function and its normal derivative may be written in terms of the complete elliptic integral of the first kind and its derivative [12].

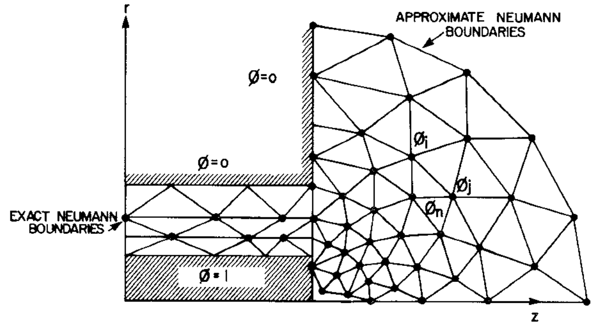


Fig. 2. Open-ended coaxial line with groundplane showing triangularization of region for solution by FEM.

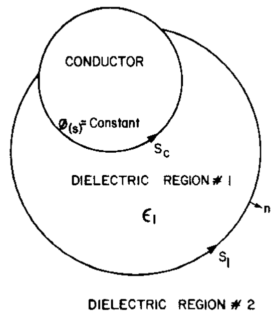


Fig. 3. Generalized configuration of an unbounded conductor-dielectric problem

The solution of (5) and (6) for the unknown surface charge distribution $\sigma(s)$ with a known potential distribution $\phi(s)$ proceeds by dividing the surface into subsections and assuming a uniform charge density of unknown amplitude on each subsection. Next, the discretized integral equations are enforced at the midpoint of each subsection, producing a system of algebraic equations for the unknown charge-pulse amplitudes. This is equivalent to using pulse expansion and Dirac weighting functions in the MOM [13].

In order to approximate an infinite line in the negative $z$-direction (see Fig. 2), the method of images was used to solve for the charge on the real conductors and interfaces and their mirror image about $z=0$. This insures an almost uniform charge distribution inside the line far from the aperture. Numerically, this involved adding a term to the Green's function to account for the presence of image charges; however, it does not affect the number of unknowns to be solved.

For both the MOM and the FEM, the resulting capacitance possesses a component due to the TEM capacitance of an infinitely long line. The TEM capacitance, given by

$$C_{\text{TEM}}=\frac{2\pi\epsilon_{\text{line}}\Delta l}{\ln(b/a)} \tag{7}$$

where $\Delta l$ is the length of line, must be subtracted from the result in order to yield the net fringing capacitance.

## III. Numerical Results

For comparison with the analytical expression for the total fringing capacitance found in [8], the configuration of a 50-Ω air line opening into a groundplane and air-dielec-

TABLE I
COMPARISON OF TOTAL CAPACITANCE OBTAINED FROM FEM AND MOM

| | Ref. [9] | FEM | MOM | Measured [4] |
|---|---|---|---|---|
| $\frac{C_T}{\epsilon_0 (b-a)}$ | 4.295 | 4.311 | 4.076 | 3.92 |

tric was solved using both methods. The ratio of outer- to inner-conductor radii for this type of line is $b/a = 2.3$ and the groundplane radius was taken to be 3 times the outer-conductor radius. Using the FEM, the region of solution shown in Fig. 2 was divided into 125 triangular elements with 80 nodes. The necessary area of the half-space required to contain most of the stored energy was found to have a radius of approximately 2.5 times the outer-conductor radius. This area was determined by progressively increasing the radius of the quadrant until the change in stored energy became less than 1 percent.

In the MOM solution, the conductors were divided into 65 subsections. 16-point Legendre–Gauss quadrature was used to integrate the Green's function for calculation of the matrix elements except the diagonal ones which were calculated using a combination of analytic and numerical integration [15].

Both programs were written in double-precision Fortran, and Gauss-elimination [17] was used for the solution of the resulting system of equations. Table I compares the values of fringing capacitance from both methods with the value computed from the low-frequency asymptotic formula in Marcuvitz [8].

The values of capacitance given in Table I and elsewhere are normalized to the free-space permittivity $\epsilon_0$ and aperture dimension $(b-a)$. Thus the results in Table I are unitless quantities and pertain to any size of open-ended 50-Ω air line.

Calculations of the fringing capacitance of 50-Ω teflon dielectric lines (identical to Fig. 1) were performed for a range of half-space permittivities $1 < \epsilon < 60$. These lines are available commercially in sizes ranging from 0.5 mm (0.02″) to 6 mm (0.25″) in diameter. The ratio of outer-conductor inner-radius to inner-conductor radius is $b/a = 3.27$ and outer-conductor outer-radius to inner-conductor radius is $c/a = 3.95$, while the line dielectric constant is $\epsilon_{\text{line}} = 2.05$.

For the FEM, 156 triangles and 96 nodes were used, while in the MOM the conductors and interface were divided into 66 and 12 subsections, respectively. Values for the normalized fringing capacitance $C(\epsilon)/\epsilon_0(b-a)$ as a function of $\epsilon$ are presented in Table II, while values of the two linear model parameters $C_f/\epsilon_0(b-a)$ and $C_0/\epsilon_0(b-a)$ are shown plotted versus $\epsilon$ in Fig. 4. For comparison, measured values are also indicated where applicable.

## IV. DISCUSSION

From the results in Table I corresponding to an open-ended air line with a groundplane, the two numerical methods gave values of normalized fringing capacitance within 5 percent of the value computed from the formula in [8] with the FEM giving the closest value. On the other

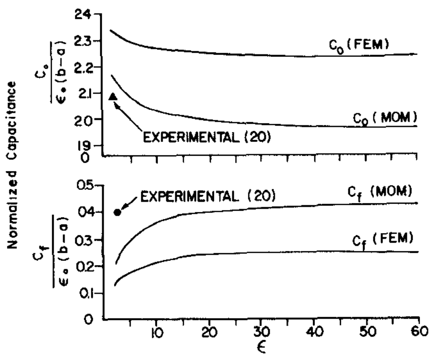


Fig. 4. Normalized $C_f$ and $C_0$ versus $\epsilon$ for 50-Ω teflon dielectric lines.

TABLE II
NORMALIZED FRINGING CAPACITANCE VERSUS $\epsilon$ (FEM AND MOM)

| | $C(\epsilon)/\epsilon_0(b-a)$ | | |
|---|---|---|---|
| $\epsilon$ | FEM | MOM | Measured |
| 1.0 | 2.48 | 2.38 | 2.42 |
| 2.0 | 4.83 | 4.56 | ---- |
| 5.0 | 11.67 | 10.72 | ---- |
| 10.0 | 22.88 | 20.62 | ---- |
| 20.0 | 45.15 | 40.11 | ---- |
| 40.0 | 89.60 | 78.85 | ---- |
| 60.0 | 134.02 | 117.53 | ---- |

hand, the MOM result is closer to the measured value reported for a 14-mm air line [4].

For the case of an open-ended teflon-filled line, the MOM gave consistently smaller values of fringing capacitance over the whole range of $\epsilon$ (Table II). When the two parameters of the linear model $C_f$ and $C_0$ are calculated according to Section II-A using the data in Table II, it is seen that both parameters vary with $\epsilon$, especially for small $\epsilon$. Also, as a result of the way in which they were defined and the consistently larger values of $C(\epsilon)$ produced by the FEM, it may be seen (Fig. 4.) that the FEM gives larger values of $C_0$ and smaller values of $C_f$ than the MOM over the range of $\epsilon$. In Fig. 4, the values of $C_f$ and $C_0$ computed from the MOM data for $\epsilon = 2$ are closer to the measured values reported in [20] than for the FEM.

In view of the close correspondence between the MOM results and measured values, it is felt that the results obtained from the MOM are more accurate than the FEM. Although no quantitative analyses of the errors in both methods were performed, several observations during the course of the work corroborate this conclusion. It was found that the FEM converged rather slowly as the number of elements increased, whereas the MOM converged quickly with an increasing number of subsections. Also, the error introduced by truncating the region of solution in the FEM may lead to a cancellation of errors since, for the functional used in this work, the FEM should give an upper bound for the capacitance.

In terms of the linear model for the fringing capacitance as a function of the permittivity, it may be seen from Fig. 4 that the use of such a model is a good approximation for large permittivities since $C_f$ and $C_0$ are relatively constant in this range. For small permittivities, say $\epsilon < 10$, the linear model is not such a good approximation since $C_f$ and $C_0$ vary with $\epsilon$, although the percentage variation in $C_0$ is relatively small. This fact together with the fact that $C_f$ is small compared to $C_0$ enables the linear model to be used for all practical purposes for small values of permittivity.

## V. Conclusion

The numerical analysis of the static fringing capacitance of an open-ended coaxial line in contact with a dielectric has been presented. This structure finds practical applications as a sensor for *in vivo* permittivity measurements at radio and microwave frequencies. The numerical values of the fringing capacitance, obtained from an application of the FEM and the MOM, were used to examine the validity of the two-capacitance or linear model relating the sample permittivity to the fringing capacitance. The results showed the linear model to be a good approximation for large permittivities such as those encountered in biological materials. The two methods also agreed with measured values of fringing capacitance reported in the literature.

For smaller permittivities (i.e., $\epsilon < 10$), a more accurate model is required as evidenced by the variation of the linear model parameters with $\epsilon$ over this range.

## Acknowledgment

Valuable and stimulating discussion with Dr. G. I. Costache from Bell-Northern Research, Ottawa, are gratefully acknowledged.

## References

[1] M. A. Stuchly and S. S. Stuchly, "Coaxial line reflection methods for measuring dielectric properties of biological substances at radio and microwave frequencies—A Review," *IEEE Trans. Instrum. Meas.*, vol. IM-29, no. 3, pp. 176–183, Sept. 1980.

[2] J. R. Mosig, J. C. E. Besson, M. Gex-Fabry, and F. E. Gardiol, "Reflection of an open-ended coaxial line and application to nondestructive measurement of materials," *IEEE Trans. Instrum. Meas.*, vol. IM-30, no. 1, Mar. 1981.

[3] E. C. Burdette, F. L. Cain, and J. Seals, "*In vivo* probe measurement technique for determining dielectric properties at VHF through microwave frequencies," *IEEE Trans. Microwave Theory Tech.*, vol. MTT-28, Apr. 1980.

[4] G. B. Gajda, "A method for the measurement of permittivity at radio and microwave frequencies," in *IEEE Int. Electrical, Electronics Conf. and Exposition, Conf. Dig.*, (Toronto, Canada), Oct. 2–4, 1979.

[5] M. A. Stuchly, M. M. Brady, S. S. Stuchly, and G. Gajda, "Equivalent circuit of an open-ended coaxial line in a lossy dielectric," *IEEE Trans. Instrum. Meas.*, vol. IM-31, pp. 116–119, June 1982.

[6] M. M. Brady, S. A. Symons, and S. S. Stuchly, "Dielectric behavior of selected animal tissues *in vitro* at frequencies from 2 to 4 GHz," *IEEE Trans. Biomed. Eng.*, vol. BME-28, Mar. 1981.

[7] H. Levine and C. H. Papas, "Theory of the circular diffraction antenna," *J. Appl. Phys.*, vol. 22, no. 1, Jan. 1951.

[8] N. Markuvitz, *Waveguide Handbook*. Boston, MA: Dover.

[9] J. Galejs, *Antennas in Inhomogeneous Media*. Oxford: Pergammon, 1969, pp. 39—43.

[10] A. Wexler, "Computation of electromagnetic fields," *IEEE Trans. Microwave Theory Tech.* (special issue on Computer-Oriented Microwave Practices), vol. MTT-17, pp. 416–439, Aug. 1969.

[11] B. H. McDonald, M. Friedman, and A. Wexler, "Variational solution of integral equations," *IEEE Trans. Microwave Theory Tech.*, vol. MTT-22, pp. 237–248, Mar. 1974.

[12] J. Daffe and R. G. Olsen, "An integral equation technique for solving rotationally symmetric electrostatic problems in conducting and dielectric material," *IEEE Trans. Power Apparatus Systems*, vol. PAS-98, no. 5, pp. 1609–1615, Sept./Oct. 1979.

[13] R. F. Harrington, *Field Computation by Moment Methods*. New York: Macmillan, 1968.

[14] G. H. Costache, M. Slanina, and E. R. Della-Giacomo, "Finite element method used to some axisymmetrical insulation problems," *Rev. Roum. Sci. Tech., Ser. Electrotech. Energ.*, vol. 20, no. 4, pp. 475–481, Bucharest, 1975.

[15] G. Gajda, "Numerical analysis of *in vivo* dielectric sensors," M.A.Sc. thesis, University of Ottawa, Ottawa, Canada, Apr. 1982.

[16] I. Stegun and A. Abrahamowitz, *Tables of Mathematical Functions*. Washington, DC: National Bureau of Standards, 1964, pp. 589–592.

[17] A. Ralston, *A First Course in Numerical Analysis*. New York: McGraw-Hill, 1965, pp. 87–90.

[18] E. Tanabe and W. T. Joines, "A nondestructive method for measuring the complex permittivity of dielectric materials at microwave frequencies using an open transmission line resonator," *IEEE Trans. Instrum. Meas.*, vol. IM-25, pp. 222–226, 1976.

[19] S. S. Stuchly, M. A. Rzepecka, and M. F. Iskander, "Permittivity measurements at microwave frequencies using lumped elements," *IEEE Trans. Instrum. Meas.*, vol. IM-23, no. 1, Mar. 1974.

[20] M. A. Stuchly, T. W. Athey, J. M. Samaras, and G. E. Taylor, "Measurements of radio frequency permittivity of biological tissues with an open-ended coaxial line: Part II, Experimental results," *IEEE Trans. Microwave Theory Tech.*, vol. MTT-30, pp. 87–92, Jan. 1982.

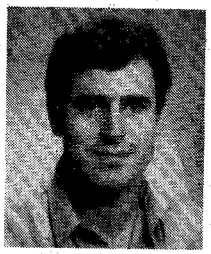

**Gregory B. Gajda** was born in Lachine, Quebec, Canada, on February 3, 1955. He received the B.Sc. degree from the University of Guelph, Guelph, Ontario, in 1977, the B.A.Sc. and M.A.Sc. degrees in electrical engineering from the University of Ottawa, Ottawa, Ontario, in 1979 and 1982, respectively.

He is presently with the Communication Research Centre in Ottawa, Canada.

**Stanislaw S. Stuchly** (M'70–SM'72) was born in Lwow, Poland, on November 20, 1931. He received the B.Sc. degree from the Technical University, Gliwice, Poland, and the M.Sc. degree from the Warsaw Technical University, both in electrical engineering, in 1953 and 1958, respectively, and the Ph.D. degree from the Polish Academy of Sciences, Warsaw, Poland, in 1968.

From 1953 to 1959 he was a Research Engineer in the Industrial Institute for Telecommunications, Warsaw, Poland, engaged in research in the field of radar and microwave theory and technique. From 1959 to 1963 he was with the Warsaw Technical University as an Assistant Professor working in the field of microwave measurements. In 1963 he joined UNIPAN–Scientific Instruments, Subsidiary of the Polish Academy of Sciences, as a Manager of the Microwave Instruments Division. In 1970 he immigrated to Canada. From 1970 to 1976 he was with the University of Manitoba, Winnipeg, Canada, as an Associate Professor in the Department of Agricultural Engineering and Electrical Engineering. Since 1977 he has been with the Department of Electrical Engineering, University of Ottawa, Canada, where he is presently a Professor and teaches courses and carries out research in the field of microwave theory and techniques as well as digital instrumentation and applications of computers. He is also a nonresident Professor at Carleton University in Ottawa. He is the author of over 80 scientific papers in the field of microwave theory and techniques as well as analog and digital instrumentation and holds 18 patents.